Surface oxides of the oxygen–copper system: Precursors to the bulk oxide phase?

Aloysius Soon [a,*], Mira Todorova [a], Bernard Delley [b], Catherine Stampfl [a]

[a] *School of Physics, The University of Sydney, Sydney 2006, Australia*
[b] *Paul-Scherrer-Institut, CH-5232, Villigen PSI, Switzerland*

Abstract

To gain an initial understanding of the copper-based catalysts in commercially important chemical reactions such as the oxygen-assisted water–gas shift reaction, we performed density-functional theory calculations, investigating the interaction of oxygen and copper, focusing on the relative stability of surface oxides and oxide surfaces of the O/Cu system. By employing the technique of ''*ab initio* atomistic thermodynamics'', we show that surface oxides are only metastable at relevant pressures and temperatures of technical catalysis, with no stable chemisorption phase observed even at very low coverage. Although exhibiting only metastability, these surface oxides resemble the bulk oxide material both geometrically and electronically, and may serve as a precursor phase before onset of the bulk oxide phase. Having identified the bulk oxide as the most stable phase under realistic catalytic conditions, we show that a $Cu_2O(111)$ surface with Cu vacancies has a lower free energy than the stoichiometric surface for the considered range of oxygen chemical potential and could be catalytically relevant.
© 2007 Elsevier B.V. All rights reserved.

1. Introduction

The basic interaction between oxygen and metal surfaces is crucial to the fundamental understanding of the role of oxygen in a number of important technological processes, such as oxidation, corrosion and heterogeneous catalysis [1,2]. Many recent studies have shown that oxygen/transition metal (O/TM) systems exhibit a rich and complex surface phase space depending upon, e.g., pressure, temperature, and stoichiometry [1–16]. Clearly, having a precise knowledge of the detailed atomic structure is central in improving the performance of existing catalysts as well as developing new ones.

Increased awareness of clean energy technology in recent years has brought about a renewed interest in the water–gas shift (WGS) reaction in relation to fuel-cell tech-

nologies, where hydrogen is produced via partial oxidation and steam reforming of hydrocarbons and methanol [17]. Copper-based catalysts are known to be catalytically active for methanol synthesis, partial oxidation of methanol and the WGS reaction. The active site, the role of support oxides, and each detailed reaction mechanism are still however not well known or understood.

As a first step towards gaining insight into the microscopic mechanisms involved in these technologically important reactions, it is helpful to investigate the interaction of O with Cu and the formation of oxide structures [3]. In the present work, we focus on the (111) surface of Cu and report results of first-principles calculations for the relative stability of surface oxides, and oxide surfaces, with the former being thin oxidic structures formed on the copper metal surface and the latter cleaved crystallographic surfaces of the bulk oxide material. The O/Cu(111) system has been investigated both theoretically [3,18] and experimentally [19–29]. Recent ultra-high vacuum scanning

tunneling microscopy experiments [19] have shown that oxidation of the Cu(1 1 1) surface is extremely complex. Observed surface geometries are described as a $(\sqrt{73}R\,5.8° \times \sqrt{21}R\,10.9°)$ structure (also known as the "*44*"-structure) and a $(\sqrt{13}R\,46.1° \times 7R\,21.8°)$ structure (also known as the "*29*"-structure). These phases are thought to resemble the primary structure of one layer of $Cu_2O(1 1 1)$, consisting of a tri-layer repeat unit with each copper layer packed in between two layers of oxygen atoms. The surface unit cell of $Cu_2O(1 1 1)$ is approximately four times the surface unit area of Cu(1 1 1) and bears a hexagonal symmetry. These factors suggest that the bulk oxide formation could be achieved via a surface oxide phase.

Recently, we investigated surface oxide formation on Cu(1 1 1) using state-of-the-art density-functional theory (DFT) calculations where we used (4×4) surface unit cells to model the above-mentioned experimentally observed structures [3]. Using the approach of "*ab initio* atomistic thermodynamics" [7,8], we identify three low-energy oxidic structures, which are energetically preferred compared to chemisorption on the surface, even at very low coverages, yet are metastable compared to the bulk cuprous oxide at relevant pressures and temperatures of technical catalysis. These surface oxides are similar to those identified from density-functional theory (DFT) calculations of the (4×4) O/Ag(1 1 1) system [9]. However, for the latter system, such structures are stable with respect to the bulk silver oxide. Recently, a new (4×4) reconstruction of the Ag(1 1 1) surface has been proposed, which shows considerably better agreement with experimental results than all previously considered models [4,5]. Being in the same base metal group in the periodic table, we investigate in the present paper the relative stability of this structure for the O/Cu(1 1 1) system.

As mentioned above, the bulk cuprous oxide phase is thermodynamically stable at relevant catalytic conditions. From the experimental literature, it is often reported that a "$Cu_2O(1 1 1)$"-like oxidic structure forms on an oxidized Cu(1 1 1) surface [19,27,29], hence as a first step, we investigate the relative stability of various terminations of bulk $Cu_2O(1 1 1)$ under relevant pressure and temperature conditions. Our results show a preference for non-stoichiometric (Cu-lean) defected surface.

2. Methodology

All the DFT calculations are performed using the generalized gradient approximation of Perdew, Burke and Ernzerhof [30] for the exchange–correlation potential as implemented in the $DMol^3$ code. The $DMol^3$ method is an all-electron code, which employs fast converging three-dimensional numerical integration to calculate the matrix elements occurring in the Ritz variational method. More details of the $DMol^3$ code can be found elsewhere [31].

All surface structures are modeled in a supercell geometry, employing a symmetric slab consisting of five (1 1 1) Cu layers, with the oxidic structures constructed on both sides. A vacuum region of 25 Å ensures the decoupling of repeated slabs. The surface oxide layer and two outermost Cu layers are fully relaxed. The wave-functions are expanded in terms of a double-numerical quality localized basis set with a real space cutoff of 9 Bohr. Brillouin-zone integrations are performed using a $(12 \times 12 \times 1)$ Monkhorst–Pack grid with 19 **k** points in the irreducible Brillouin-zone (IBZ) of a (1×1) cell and a thermal broadening of 0.1 eV. To obtain the same sampling of the reciprocal space for larger surface cells, this number is reduced accordingly. To model the $Cu_2O(1 1 1)$ surfaces, we employ a (1×1) surface unit cell and use a $(8 \times 8 \times 1)$ Monkhorst–Pack grid with 10 **k** points in the IBZ. We use a 15-atomic layer slab, separated by a vacuum region of 33.5 Å, and fully relax the 12 outermost layers. The high accuracy of the basis set is described in Ref. [3].

To take into consideration realistic experimental conditions, the effect of temperature and pressure is included by taking into account the surrounding gas phase in terms of "*ab initio* atomistic thermodynamics" [7,8]. This approach allows the determination of the lowest-energy surface structure, for given conditions of a surrounding gas phase. More details of the methodology can be found elsewhere [2,3].

3. Results and discussion

3.1. Surface oxides

In our earlier publication [3], we carried out detailed DFT calculations to investigate on-surface and sub-surface adsorption of O on Cu(1 1 1), as well as the stability of surface oxide structures. To replicate the so-called "*44*"- and "*29*"-structures, we used a (4×4) supercell to model various possible configurations of different oxygen content. As the surface area of a (1×1) unit cell of $Cu_2O(1 1 1)$ is approximately four times that of Cu(1 1 1), the (4×4) supercell is deemed a good starting point to mimic these superoxide structures seen experimentally. Our findings may be summarized as follows: For conditions typical of technical catalysis (e.g., $p = 1$ atm, $T = 600$ K), the bulk oxide is thermodynamically most stable; however, if formation of the fully oxidized surface is prevented due to kinetic hindering, thin surface oxides are found to be energetically preferred compared to chemisorption on the surface, even at very low coverage. The main results are displayed in Fig. 1A, which shows the Gibbs free energy of the lowest-energy structures versus the oxygen chemical potential [8]. By including the effects of pressure and temperature through the dependence of the oxygen molecule, we correlate the oxygen chemical potential with a pressure scale for selected temperatures. For reference, we have included the result for chemisorption of O on Cu(1 1 1) at coverage 0.25 ML, as calculated using a (2×2) surface unit cell. It can be seen that for values of the oxygen chemical potential $(\Delta\mu_O)$ of less than -1.65 eV, the clean Cu(1 1 1) surface is
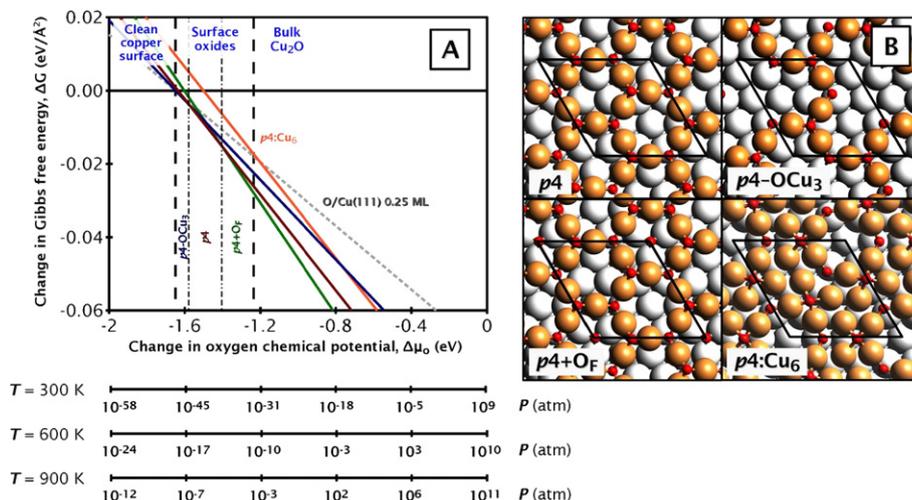
Fig. 1. (A) Calculated Gibbs free energy of adsorption (relative to the clean Cu(111) surface) of low-energy oxidic surface structures with varying oxygen chemical potential $\Delta\mu_O$ (given with respect to half the total energy of the O_2 molecule). (B) Optimized surface oxide structures of the O/Cu(111) system. The surface unit cell is indicated. The underlying Cu substrate layer is shown as pale grey spheres, with the Cu atoms in the oxide layer, medium grey (orange). Oxygen atoms are denoted by small grey (red) spheres. (For interpretation of the references to color in Figs. 1, 2 and 3 legend, the reader is referred to the web version of this article.)

thermodynamically most stable. For higher values of $\Delta\mu_O$, from -1.65 to -1.24 eV, the so-called "$p4$-OCu_3", "$p4$" and "$p4 + O_F$" structures are the most favorable. The atomic geometry of these configurations is shown in Fig. 1B and closely resemble the (111) surface of bulk cuprous oxide, Cu_2O (see Fig. 2B). At certain temperatures and pressures, these surface oxides are predicted to be stable before the onset of the bulk oxide phase at

$\Delta\mu_O = -1.24$ eV (i.e., for pressures and temperatures of e.g., $T = 600$ K for $p < 10^{-10}$ atm, or $T = 900$ K for $p < 10^{-3}$ atm etc). Hence, one can speculate that the formation of the bulk Cu_2O phase could possibly be achieved via a precursor surface oxide phase(s).

We now consider the relative stability of the recently reported "new" (4×4)-O/Ag(111) structure [4,5] in relation to the other O/Cu surface oxide structures we have
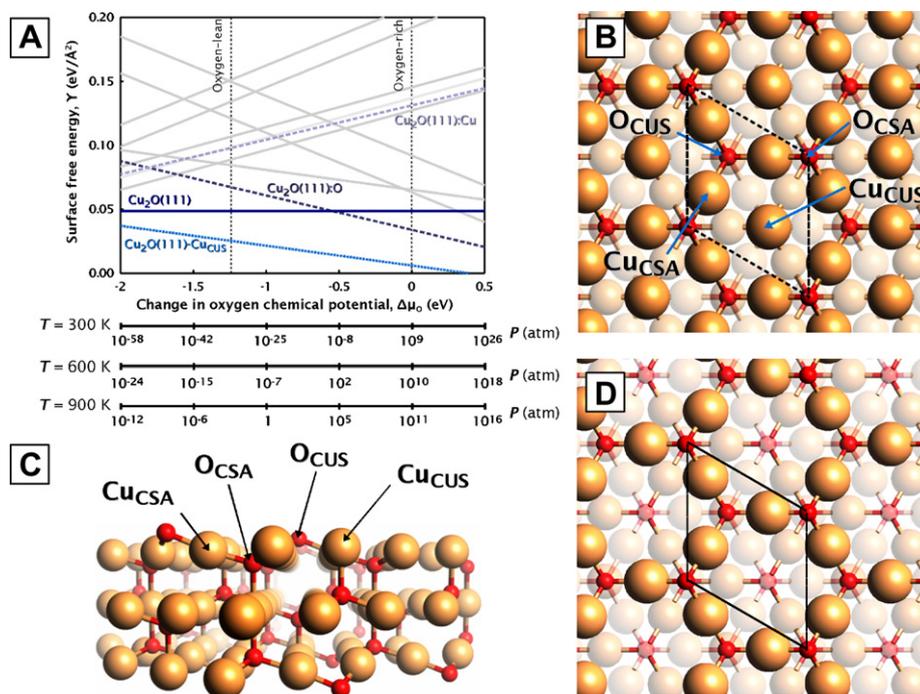

Fig. 2. The calculated surface free energy for the various $Cu_2O(111)$ surface terminations as a function of oxygen chemical potential (given with respect to half the total energy of O_2) is shown in (A). (B) and (C) show the top and side view of the optimized atomic structure of $Cu_2O(111)$, respectively. (D) shows the top view of the low-energy $Cu_2O(111)$–Cu_{CUS} structure. The upper Cu atoms are shown as large medium grey (orange) spheres, with the oxygen atoms denoted by small grey (red) spheres. The labels "CSA" and "CUS" stand for coordinatively saturated, and coordinatively unsaturated, respectively.

investigated. The atomic structure of this new phase is shown in Fig. 1B and labeled "*p*4:Cu₆", reflecting the fact that it has six additional Cu atoms in the surface unit cell as compared to the *p*4 structure. We find that the average oxygen binding energy is 1.50 eV, which is 0.14 eV less favorable that the *p*4 structure, which has the same oxygen coverage. Hence this new "oxide" is unlikely to be considered as a precursor oxide phase for the O/Cu(1 1 1) system. Table 1 lists the average oxygen binding energies of our previously reported surface oxide structures for comparison.

3.2. Cu₂O(1 1 1) oxide surfaces

We now turn to investigate the surface free energies for different (1 1 1) surface terminations of bulk Cu₂O. The stoichiometric surface atomic geometry is shown in Figs. 2B and 2C. We investigate many possible surface structures by generating vacancies, anti-sites, interstials and adsorption of O or Cu atoms. The Cu-terminated and O-terminated Cu₂O(1 1 1) surfaces are also considered. By removing O_{CUS} from the stoichiometric surface, the Cu-terminated surface is generated (labeled as Cu₂O(1 1 1):Cu) and adding an O atom on top of the Cu_{CUS} of the stoichiometric surface, one obtains the O-terminated Cu₂O(1 1 1) (labeled as Cu₂O(1 1 1):O), making it fully-coordinated in this case.

To determine the relative stability of the various oxide terminations, we calculate the surface free energy,

$$\gamma(p, T) = \frac{1}{A}(G - N_{Cu}\mu_{Cu} - N_O\mu_O), \quad (1)$$

where N_{Cu} and N_O are the number of oxygen and copper atoms, and A is the surface area. The p and T dependence is given by μ_O, the oxygen chemical potential, i.e., by the O₂ gas phase. We refer to Ref. [7,8] for details. G is the free energy of the stoichiometric Cu₂O slab, and μ_{Cu}, the copper atom chemical potential, is taken as $\frac{1}{2}(g_{Cu_2O} - \mu_O)$, where g_{Cu_2O} is the free energy per Cu₂O unit in the bulk phase. Both G and g are approximated as the respective calculated total energy. The "oxygen-rich" limit corresponds to $\mu_O = \frac{1}{2}E_{O_2}$, where E_{O_2} is the total energy of the oxygen molecule. For more details, we refer to Ref. [6].

Table 1
Average binding energies, E_b (per O atom), of surface oxide structures (with respect to half the calculated binding energy of O₂) at corresponding oxygen coverages. The O:Cu ratio is the ratio of the number of oxygen atoms to that of copper atoms in the surface oxide layer and the oxide surfaces

Structures	Coverage (ML)	O:Cu ratio	E_b (eV)
Chemisorbed O/Cu	0.250	–	1.65
*p*4-OCu₃	0.313	0.833	1.65
*p*4	0.375	0.667	1.64
*p*4:Cu₆	0.375	0.500	1.50
*p*4 + O_F	0.438	0.778	1.60
Cu₂O(1 1 1)	–	0.500	–
Cu₂O(1 1 1)–Cu_CUS	–	0.667	–

The calculated surface free energies of all considered configurations are shown in Fig. 2A. It can be seen that most of the structures are unfavorable (pale grey lines) when compared to the stoichiometric surface. However, importantly, for one case, "Cu₂O(1 1 1)–Cu_CUS" in which the coordinatively unsaturated copper atom, Cu_{CUS}, is removed from the surface unit cell of the stoichiometric structure, the energy is notably lower (see Fig. 2D). This structure becomes greatly stabilized at high oxygen chemi-
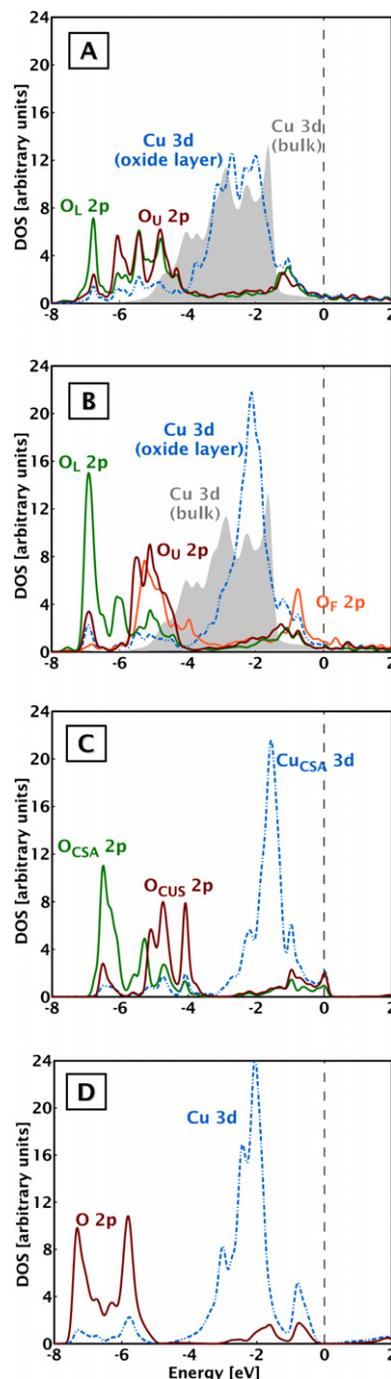

Fig. 3. Projected density-of-states (PDOS) for selected surface structures (A) *p*4:Cu₆, (B) *p*4 + O_F, (C) Cu₂O(1 1 1)–Cu_CUS and (D) bulk Cu₂O. The Fermi energy is indicated by the vertical dashed line.

cal potential and could possibly play a key role in certain catalytic reactions.

Full details of the nature of all surface terminations considered are described in Ref. [32].

3.3. Density of states

Having discussed the energetics and geometric structures of the surface oxides and (111) oxide surfaces, we now consider the electronic structure by calculating the projected density-of-states (PDOS). Fig. 3 shows the PDOS for the structures, $p4$:Cu_6, $p4 + O_F$, $Cu_2O(111)$–Cu_{CUS} and bulk Cu_2O. It can be seen that there is a significant narrowing of the $3d$ band of Cu in the $p4 + O_F$ oxide layer, closely resembling that of the bulk oxide. In contrast, the Cu $3d$ band of $p4$:Cu_6 shows a smaller narrowing, largely retaining bulk (or surface) Cu-like character. The O $2p$ bands of $p4 + O_F$ exhibit more similar features to that of the bulk oxide as compared to $p4$:Cu_6. This can be understood by consideration of the atomic structure of both surface oxides: The $p4 + O_F$ has a more open structure, hence the Cu atoms in the oxide layer have a lower coordination when compared to bulk Cu. On the other hand, the $p4$:Cu_6 oxide layer still retains a monolayer Cu(111)-like arrangement and this leads to a higher coordination as compared to $p4 + O_F$.

Turning to the lowest-energy oxide surface, $Cu_2O(111)$–Cu_{CUS}, its PDOS retains similar generic features to that of the bulk oxide. However, the centre of its Cu_{CSA} $3d$ band has shifted closer to the Fermi energy and the O $2p$ bands have also broadened, which has narrowed the gap between the Cu $3d$ and O $2p$ bands when compared to the bulk bands. This is mainly due to the O $2p$ states of the O_{CUS} atom, and is similar to the PDOS of the O_U atom (i.e., the uppermost oxygen atom) of the $p4 + O_F$ structure, both being coordinatively unsaturated. An obvious difference to the bulk PDOS is that electronic states can be seen at the Fermi energy, inducing a "metallic" character.

4. Summary and conclusion

We have investigated the atomic structure, energetics and electronic properties of surface oxides of the O/Cu(111) system, as well as various $Cu_2O(111)$ oxide surfaces. We identify a plausible precursor phase to bulk oxide formation to be $p4 + O_F$, which resembles rather closely the (111) oxide surface. The newly proposed surface oxide structure for (4×4) O/Ag(111) is found for the O/Cu(111) system to be thermodynamically unfavorable and distinctly different from its native oxide, both geometrically and electronically. The bulk oxide phase is identified as the most stable phase under realistic catalytic conditions. We have found that a defected $Cu_2O(111)$ surface, "$Cu_2O(111)$–Cu_{CUS}", involving surface copper vacancies, exhibits a lowest surface free energy for the considered range of oxygen chemical potential, and we propose it could play an important role in heterogeneous catalytic reactions.

References

[1] C. Stampfl, M.V. Ganduglia-Pirovano, K. Reuter, M. Scheffler, Surf. Sci. 500 (2002) 368.
[2] C. Stampfl, Catal. Today 105 (2005) 17.
[3] A. Soon, M. Todorova, B. Delley, C. Stampfl, Phys. Rev. B 73 (2006) 165424.
[4] M. Schmid, A. Reicho, A. Stierle, L. Costina, J. Klikovits, P. Kostelnik, O. Dubay, G. Kresse, J. Gustafson, E. Lundgren, J.N. Anderson, H. Dosch, P. Varga, Phys. Rev. Lett. 96 (2006) 146102.
[5] J. Schnadt, A. Michaelides, J. Knudsen, R.T. Vang, K. Reuter, E. Lægsgaard, M. Scheffler, F. Besenbacher, Phys. Rev. Lett. 96 (2006) 146101.
[6] W.X. Li, C. Stampfl, M. Scheffler, Phys. Rev. B 65 (2002) 075407;
W.X. Li, C. Stampfl, M. Scheffler, Phys. Rev. B 67 (2003) 045408;
W.X. Li, C. Stampfl, M. Scheffler, Phys. Rev. B 68 (2003) 165412.
[7] W.X. Li, C. Stampfl, M. Scheffler, Phys. Rev. Lett. 90 (2003) 256102.
[8] K. Reuter, M. Scheffler, Phys. Rev. B 65 (2002) 035406.
[9] A. Michaelides, K. Reuter, M. Scheffler, J. Vac. Sci. Tech. A 23 (2005) 1487.
[10] M. Todorova, W.X. Li, M.V. Ganduglia-Pirovano, C. Stampfl, K. Reuter, M. Scheffler, Phys. Rev. Lett. 89 (2002) 096103.
[11] J. Gustafson, A. Mikkelsen, M. Borg, E. Lundgren, L. Köhler, G. Kresse, M. Schmid, P. Varga, J. Yuhara, X. Torrelles, C. Quirós, J.N. Andersen, Phys. Rev. Lett. 92 (2004) 126102.
[12] E. Lundgren, G. Kresse, C. Klein, M. Borg, J.N. Andersen, M. De Santis, Y. Gauthier, C. Konvicka, M. Schmid, P. Varga, Phys. Rev. Lett. 88 (2002) 246103.
[13] E. Lundgren, J. Gustafson, A. Mikkelsen, J.N. Andersen, A. Stierle, H. Dosch, M. Todorova, J. Rogal, K. Reuter, M. Scheffler, Phys. Rev. Lett. 92 (2004) 046101.
[14] L. Zhou, S. Günther, D. Moszynski, R. Imbihl, J. Catal. 235 (2005) 359.
[15] K. Reuter, M. Scheffler, Phys. Rev. Lett. 90 (2003) 046103.
[16] P.D. Szuromi, Science 310 (2005) 1091.
[17] A.Y. Rozovskii, G.I. Lin, Top. Catal. 22 (2003) 137.
[18] Y. Xu, M. Mavrikakis, Surf. Sci. 494 (2001) 131.
[19] T. Matsumoto, R.A. Bennett, P. Stone, T. Yamada, K. Domen, M. Bowker, Surf. Sci. 471 (2001) 225.
[20] G. Ertl, Surf. Sci. 6 (1967) 208.
[21] A. Spitzer, H. Luth, Surf. Sci. 118 (1982) 136.
[22] R.W. Judd, P. Hollins, J. Pritchard, Surf. Sci. 171 (1986) 643.
[23] M.K. Rajumon, C.N.R.R.K. Prabhakaran, Surf. Sci. 233 (1990) L237.
[24] H. Niehus, Surf. Sci. 130 (1983) 41.
[25] J. Haase, H.J. Kuhr, Surf. Sci. 203 (1988) L695.
[26] B. Luo, J. Urban, J. Phys. Condens. Matter 3 (1991) 2873.
[27] R.L. Toomes, D.P. Woodruff, M. Polcik, S. Bao, P. Hofmann, K.M. Schindler, Surf. Sci. 443 (2000) 300.
[28] F. Jensen, F. Besenbacher, E. Lægsgaard, I. Stensgaard, Surf. Sci. 259 (1991) L774.
[29] S.M. Johnston, A. Mulligan, V. Dhanak, M. Kadodwala, Surf. Sci. 519 (2002) 57.
[30] J. Perdew, K. Burke, M. Ernzerhof, Phys. Rev. Lett. 77 (1996) 3865.
[31] B. Delley, J. Chem. Phys. 92 (1990) 508;
B. Delley, J. Chem. Phys. 113 (2000) 7756.
[32] A. Soon, M. Todorova, B. Delley, C. Stampfl, Phys. Rev. B 75 (2007) 125420.